Supplemental Table 1: Different RT primer designs tested during the optimization of the assays. Different combinations for placement and length of the 5′ hemiprobe (red) and 3′ hemiprobe (blue) were tested in sequential experiments. The adenosine nucleotide subject to deamination upon RNA editing is highlighted in bold print. The probe placement that was selected for all subsequent experiments is highlighted with gray shading.

Probe placement on miR-379	Efficient amplification?	Specificity	Sensitivity
UGGU**A**GACUAUGGAACGUAGG	no	n/a	n/a
UGGU**A**GACUAUGGAACGUAGG	yes	< 1%	10^3
UGGU**A**GACUAUGGAACGUAGG	yes	> 1%	n/a
UGGU**A**GACUAUGGAACGUAGG	no	n/a	n/a
UGGU**A**GACUAUGGAACGUAGG	yes	< 1%	10^3
UGGU**A**GACUAUGGAACGUAGG	yes	< 1%	10^3
UGGU**A**GACUAUGGAACGUAGG	no	n/a	n/a
UGGU**A**GACUAUGGAACGUAGG	yes	< 1%	10^2
UGGU**A**GACUAUGGAACGUAGG	yes	> 1%	n/a
UGGU**A**GACUAUGGAACGUAGG	no	n/a	n/a
UGGU**A**GACUAUGGAACGUAGG	yes	< 1%	10^2
UGGU**A**GACUAUGGAACGUAGG	yes	> 1%	n/a

Supplemental Table 2: RNA oligonucleotide sequences.

Name	Sequence
unedited miR-379-5p	5′-UGGUAGACUAUGGAACGUAGG-3′
edited miR-379-5p	5′-UGGUIGACUAUGGAACGUAGG-3′
miR-380-5p	5′-UGGUUGACCAUAGAACAUGCGC-3′
unedited miR-411-5p	5′-UAGUAGACCGUAUAGCGUACG-3′
edited miR-411-5p	5′-UAGUIGACCGUAUAGCGUACG-3′
miR-758-5p	5′-GAUGGUUGACCAGAGAGCACAC-3′

Supplemental Table 3: DNA sequences of primers and hydrolysis probes.

Type	Name	Sequence
RT primer	unedited miR-379 RT	5′-AGTCTATCATCATCAGAGCTAGAG AACCTAGCTCACCCACACTCCTAC-3′
	edited miR-379 RT	5′-AGTCCATCATCATCAGAGCTAGAG AACCTAGCTCACCCACACTCCTAC-3′
	pan-miR-379 RT	5′-ATAGTCTCATCATCAGAGCTAGAG AACCTAGCTCACCCACACTCCTAC-3′
qPCR primer	unedited miR-379 fwd	5′-GCAGTCTATCATCATCAGAGCTAG-3′
	unedited miR-379 rev	5′-GCGTGGTAGACTATGGAACG-3′
	edited miR-379 fwd (for SYBR Green-based qPCR)	5′-GCAGTCCATCATCATCAGAGCTAG-3′
	edited miR-379 fwd_short (for hydrolysis-based qPCR)	5′-AGTCCATCATCATCAGAGCTAG-3′
	edited miR-379 rev	5′-CGGGTGGACTATGGAACG-3′
	pan-miR-379 fwd	5′-GCATAGTCTCATCATCAGAGCTAG-3′
	pan-miR-379 rev-1 (higher affinity for edited miR-379)	5′-GCCTGGTGGACTATGGAACG-3′
	pan-miR-379 rev-2 (higher affinity for unedited miR-379)	5′-GCCTGGTAGACTATGGAACG-3′
hydrolysis probe	miR-379 hydrolysis probe (binds both unedited and edited RT products)	5′-(6-FAM)-AGGAGTGTG-(ZEN)-GGTGAGCTAGGTTCT-(Iowa Black FQ)-3′
RT-PCR primer	pri-miR-379 fwd	5′-TTTATGTTCACCATGTGCCTGC-3′
	pri-miR-379 rev	5′-TGCTGAAGCTAAACCACGTGTT-3′
Cloning primers	pLV-backbone_fwd	5′-TCCGGTCGACTGCAGAATTC-3′
	pLV-backbone_rev	5′-ATTCTACCGGGTAGCGAC-3′
	FLAG_fwd	5′-GAATTCTGCAGTCGACCGGA ATGGACTACAAGGACGAC-3′
	6xHis_rev	5′-TAGTCGCTACCCGGTAGAAT CTAATGGTGATGGTGATG-3′
	pLV-eGFP-PuroR_rev_SalI	5′-ATATGTCGACAGAGGGCCCGTTAGATCTC-3′
	pLV-backbone_rev_SalI	5′-ATATGTCGACATTCTACCGGGTAGCGAC-3′

Supplemental Table 4: Clinical characteristics of patients in the prostate cancer cohort. For PSA and age, the median and range are stated.

		Prostate cancer	**Benign prostatic hyperplasia**
Total number of patients		47	23
Age at TURP		75 (63-89) years	69 (56-89) years
WHO Grade	Grade I	4	-
	Grade II	20	-
	Grade III	23	-
Clinical stage	T1	9	-
	T2	21	-
	T3	13	-
	T4	3	-
	Data missing	1	
PSA at surgery		26.7 (0.2-672) ng/ml	6.6 (3-19.4) ng/ml
Metastasis	Yes	25	-
	No	8	-
	Not suspected	9	-
	Data missing	5	-

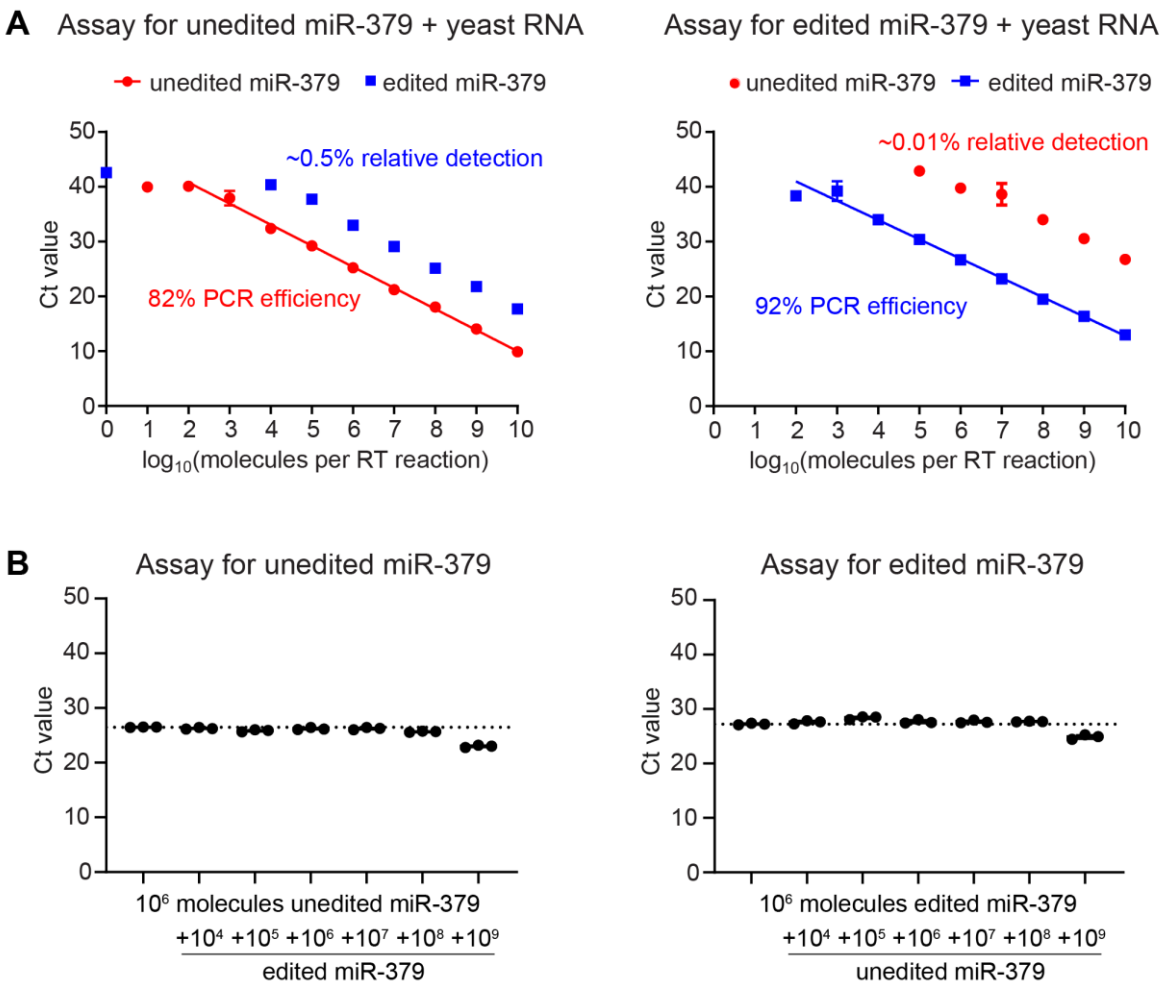

Supplemental Figure 1. Performance of the two-tailed miR-379 assays in mixtures of molecules. (**A**) Ct values for different dilutions of unedited (red circles) and edited (blue squares) miR-379 RNA oligonucleotides quantified by the two-tailed RT-qPCR assays specific for unedited (left) and edited (right) miR-379 with 100 ng yeast RNA contained in each reaction to create an artificial background. Error bars denote standard deviation; for points without error bars, the standard deviation was too small to be plotted. PCR efficiencies were calculated based on the slope. The average relative detection rate of non-target miR-379 was calculated based on the Ct difference to target miR-379. (**B**) Triplicate Ct values of mixtures containing one million molecules of target miR-379 and varying amounts of non-target miR-379 for unedited (left) and edited (right) miR-379 assays. Dotted line denotes the average Ct value of mixtures containing only the target molecule.

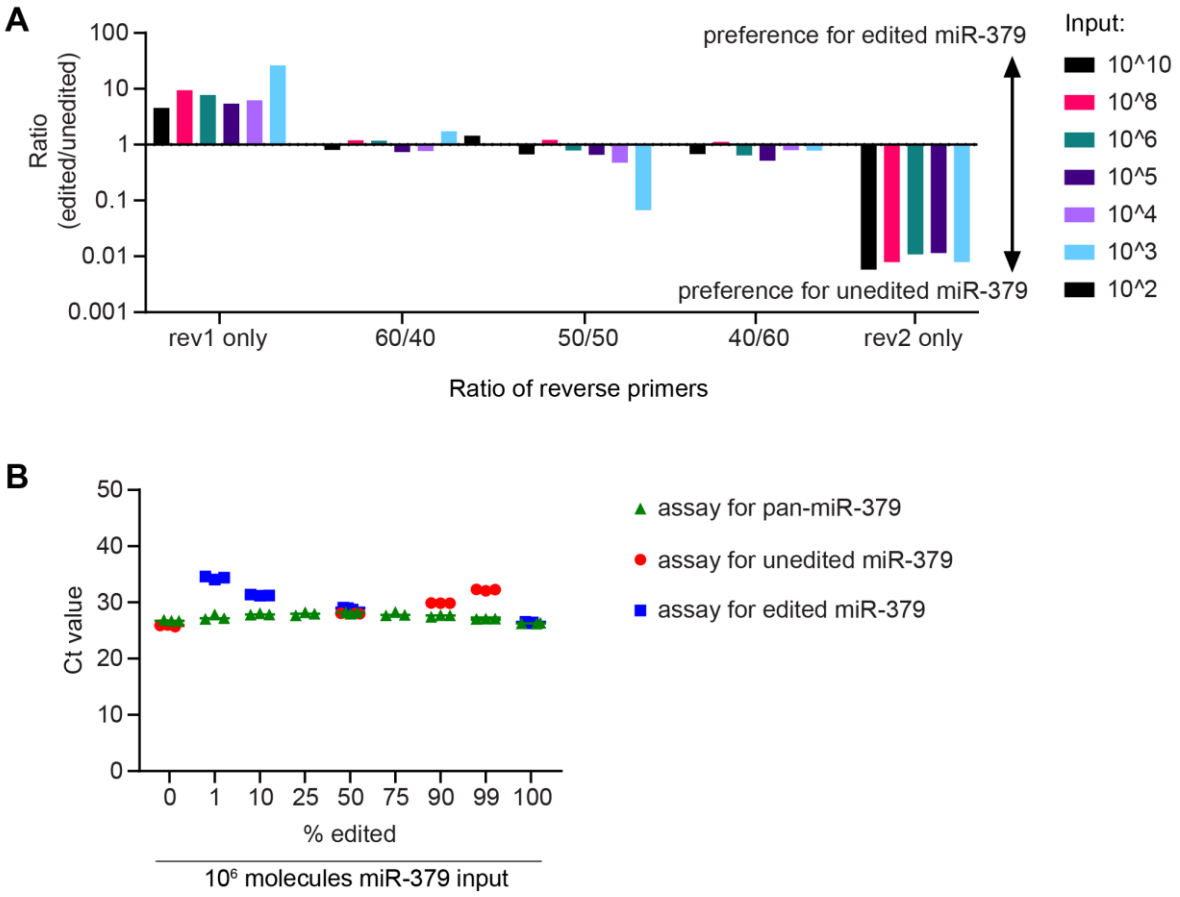

Supplemental Figure 2. Two-tailed RT-qPCR assay for pan-miR-379. (**A**) Ratio between detection of different amounts of unedited and edited miR-379 by pan-miR-379 assays using different mixtures of reverse primers. A reverse primer ratio of 60/40 was deemed optimal as the detection ratios were closest to 1 with the least bias towards one or the other isoform, and this is the ratio that was subsequently used for all experiments in the study. (**B**) Amplification of mixtures of different miR-379 isoforms. All samples contain one million molecules of miR-379, but at different ratios (indicated as the fraction of edited miR-379 along the x-axis). Green triangles indicate Ct values with pan-miR-379 assays, whereas red circles (unedited miR-379) and blue squares (edited miR-379) indicate Ct values of the same samples quantified with isoform-specific assays, demonstrating differences in isoform composition of the mixtures.

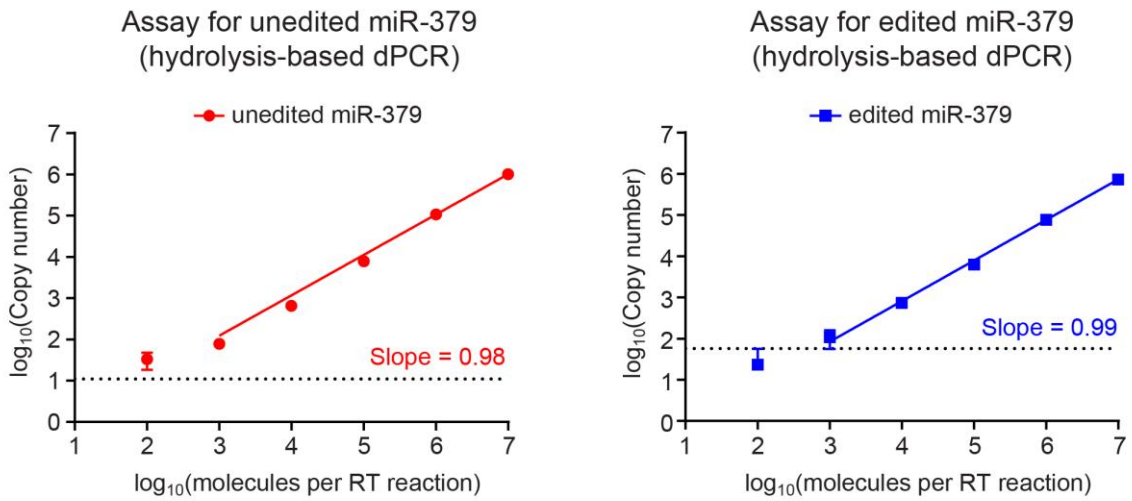

Supplemental Figure 3. Hydrolysis probe-based dPCR of different dilutions of unedited (left) and edited (right) miR-379 RNA oligonucleotides quantified by their specific two-tailed RT-qPCR assays, illustrating the dynamic range up to 10^7 molecules input. Error bars denote standard deviation; for points without error bars, the standard deviation was too small to be plotted.

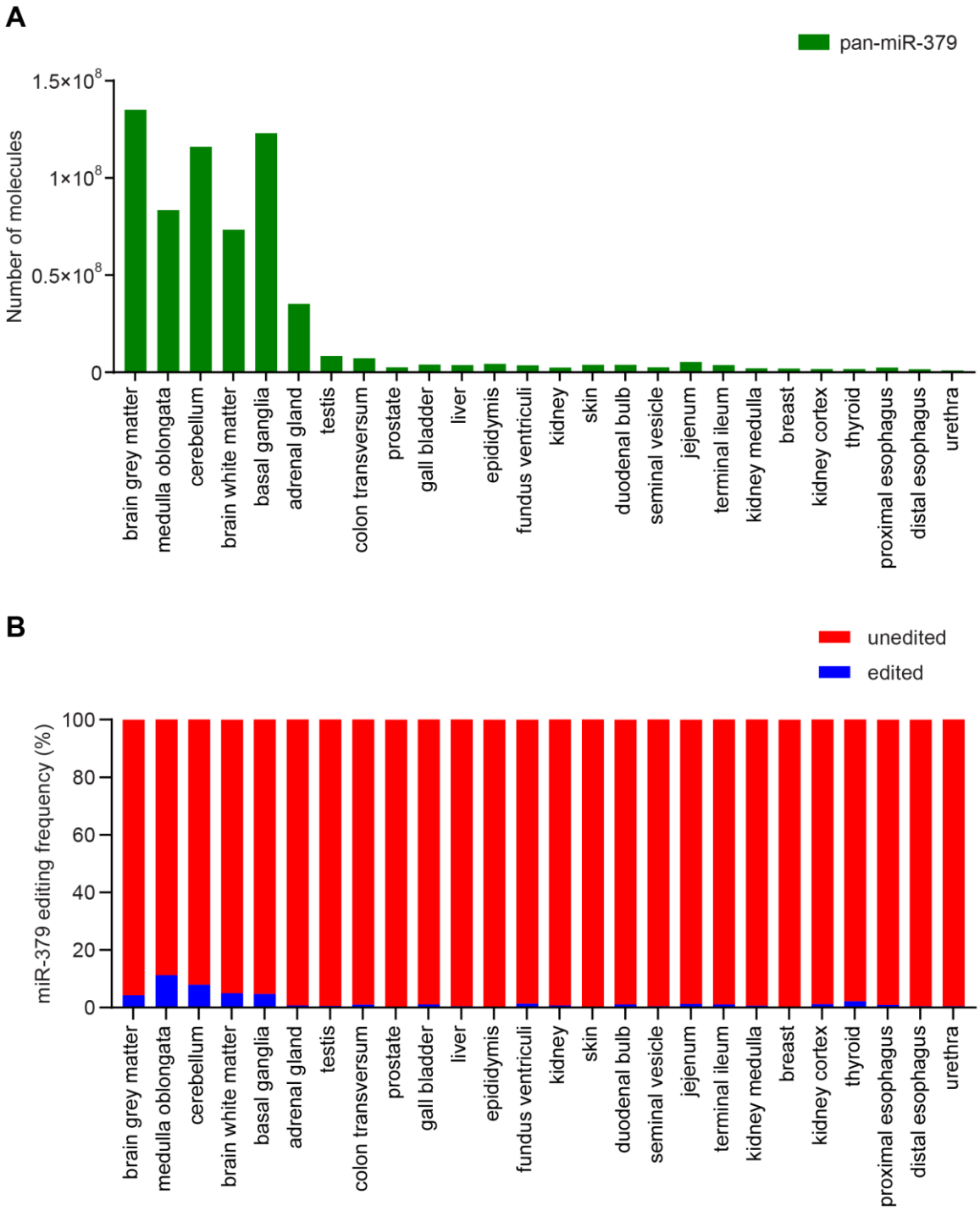

Supplemental Figure 4. (**A**) Number of molecules of pan-miR-379 in human tissues as measured by editing-independent two-tailed RT-qPCR. Absolute numbers were derived from standard curves of serially diluted RNA oligonucleotides, and normalized using the geometric mean of RNU24, RNU44, RNU48 and RNU66. (**B**) Editing frequencies of mature miR-379 in the human tissue panel. Editing frequencies were calculated based on the absolute number of edited miR-379 molecules divided by the sum of unedited and edited miR-379 molecules.

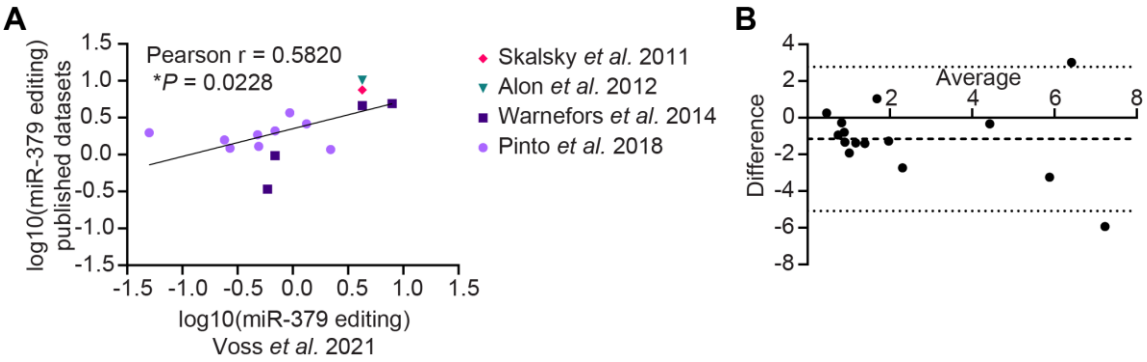

Supplemental Figure 5. Comparison of miR-379 editing frequencies in different tissues with published RNA sequencing data. (**A**) Correlation between miR-379 editing frequencies in our data and those in published RNA sequencing datasets. From Pinto *et al.*, only editing frequencies for normal tissues were used. (**B**) Bland-Altman plot for the same data as (**A**), showing the difference between editing frequencies determined by qPCR and RNA sequencing. The dashed line represents the bias, dotted lines show the limits of agreement.

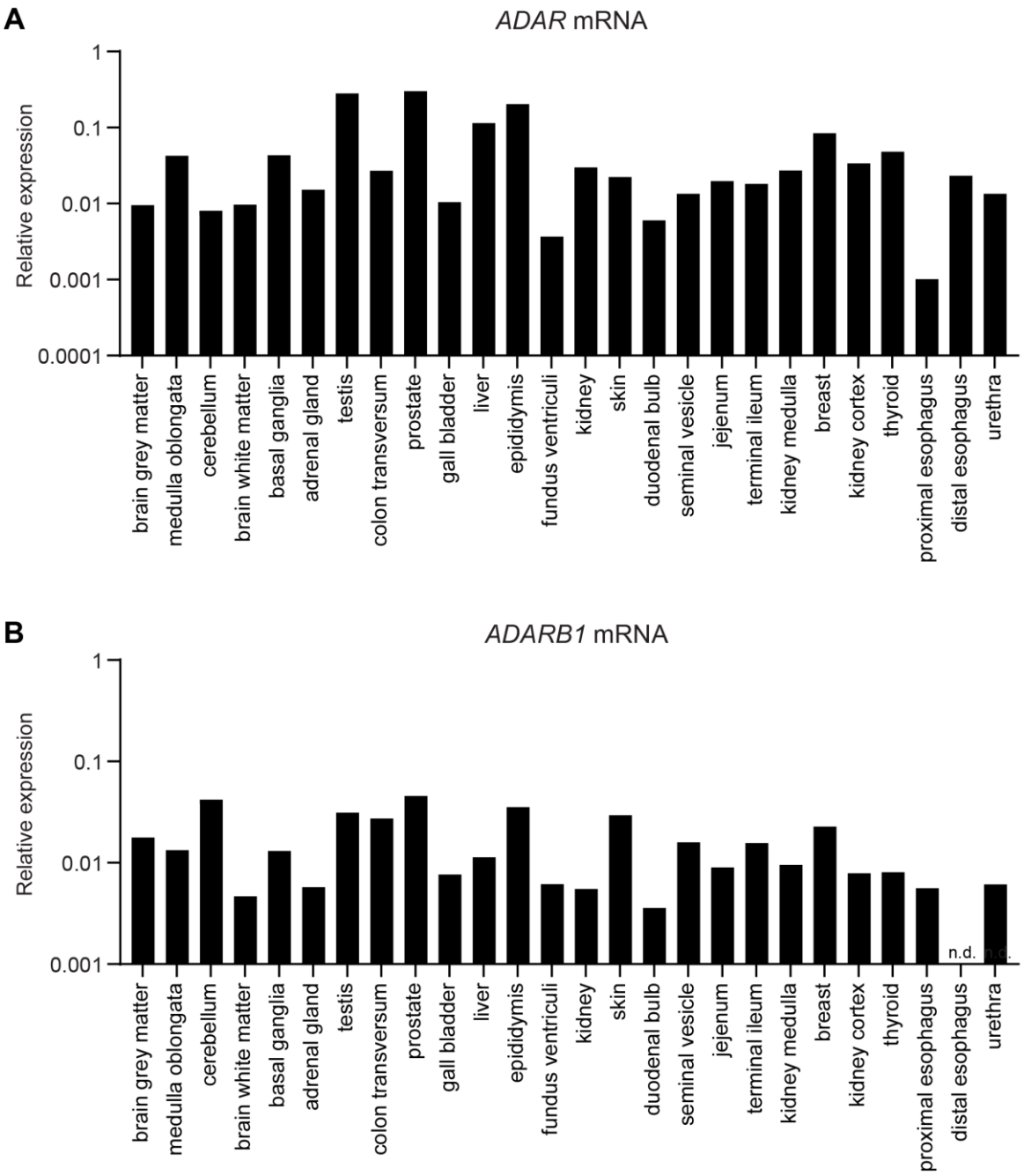

Supplemental Figure 6. (**A**) *ADAR* and (**B**) *ADARB1* mRNA expression in human tissues. Relative expression was calculated by normalization to *GUSB, PGK1* and *GAPDH* mRNAs. In distal esophagus cDNA, *ADARB1* was undetectable. n.d. = not detected.

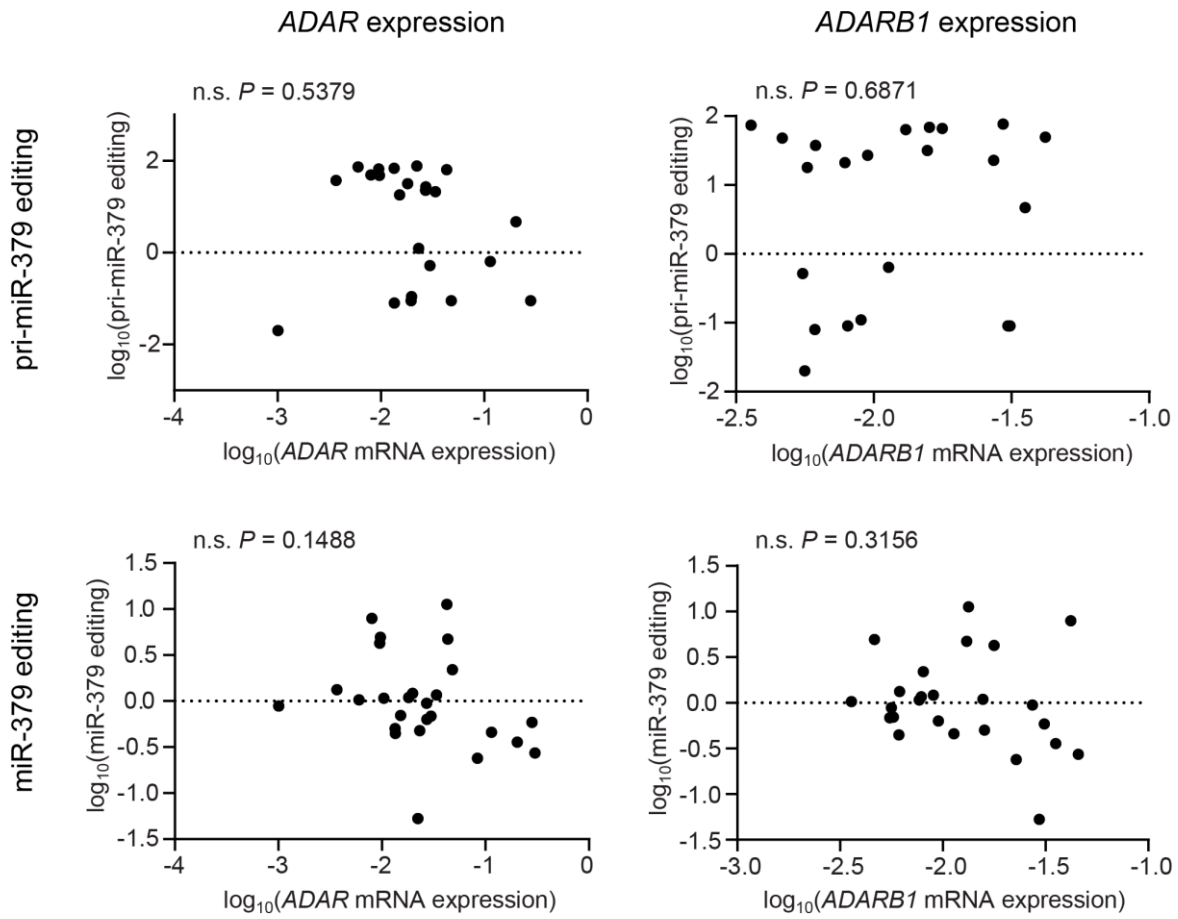

Supplemental Figure 7. Correlation analysis between pri-miR-379 (top) or miR-379 (bottom) editing frequencies and *ADAR* (left) or *ADARB1* (right) mRNA expression levels in human tissues. Variables were log-transformed to perform meaningful linear regression and Pearson correlation. n.s. = not significant.

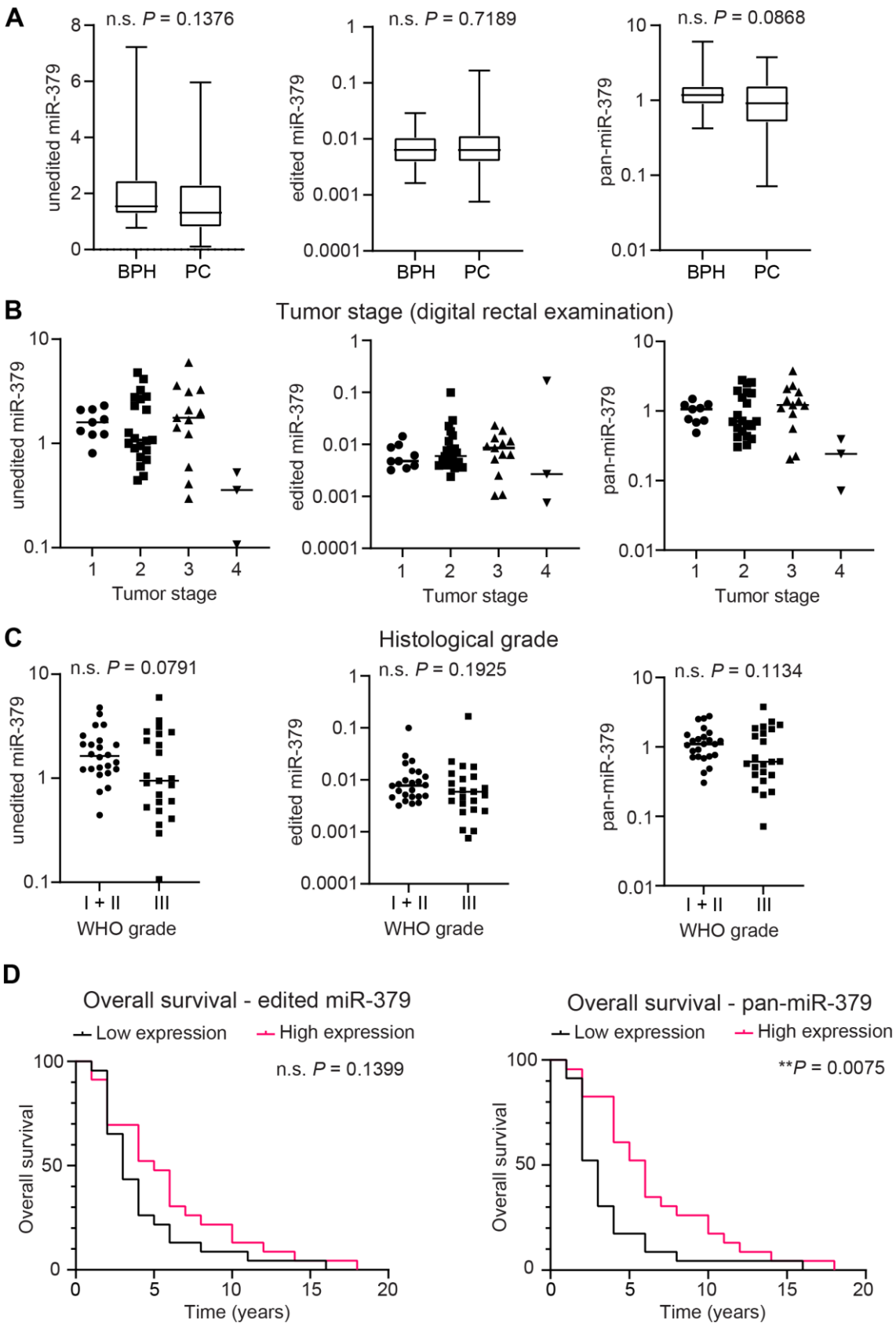

Supplemental Figure 8. (Legend on the following page)

Supplemental Figure 8. Expression of miR-379 isoforms in the PC patient cohort. (**A**) Relative expression of unedited miR-379 (left), edited miR-379 (middle) and pan-miR-379 (right) in patients with BPH (n = 23) and PC (n = 47). Expression was normalized to the geometric mean of U47, RNU48 and RNU66. Box plot marks the median and upper and lower quartiles, whiskers denote the range of values. (**B**) Relative expression of unedited miR-379 (left), edited miR-379 (middle) and pan-miR-379 (right) by tumor stage (n = 9 for T1, n = 21 for T2, n = 13 for T3, n = 3 for T4). Individual values and the median are shown. (**C**) Relative expression of unedited miR-379 (left), edited miR-379 (middle) and pan-miR-379 (right) by pathological grade (n = 4 for Grade I, n = 20 for Grade II, n = 23 for Grade III). Expression was normalized to the geometric mean of U47, RNU48 and RNU66. Individual values and the median are shown. (**D**) Survival analysis by edited miR-379 (left) and pan-miR-379 (right). Group comparisons were done by Mann-Whitney U tests. For survival analysis, patients were divided at the median by expression (n = 23 in each group), and curves were compared using log-rank test. n.s. = not significant.

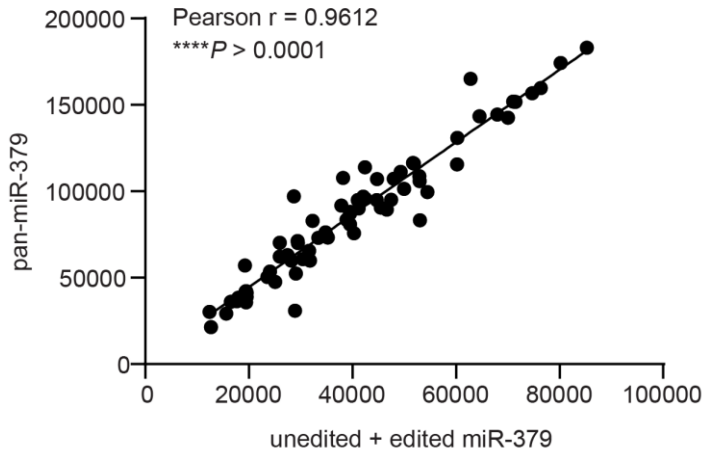

Supplemental Figure 9. Correlation between the sum of unedited and edited miR-379 molecules and pan-miR-379 molecules (n = 70). The *P*-value was calculated by linear regression and Pearson correlation.

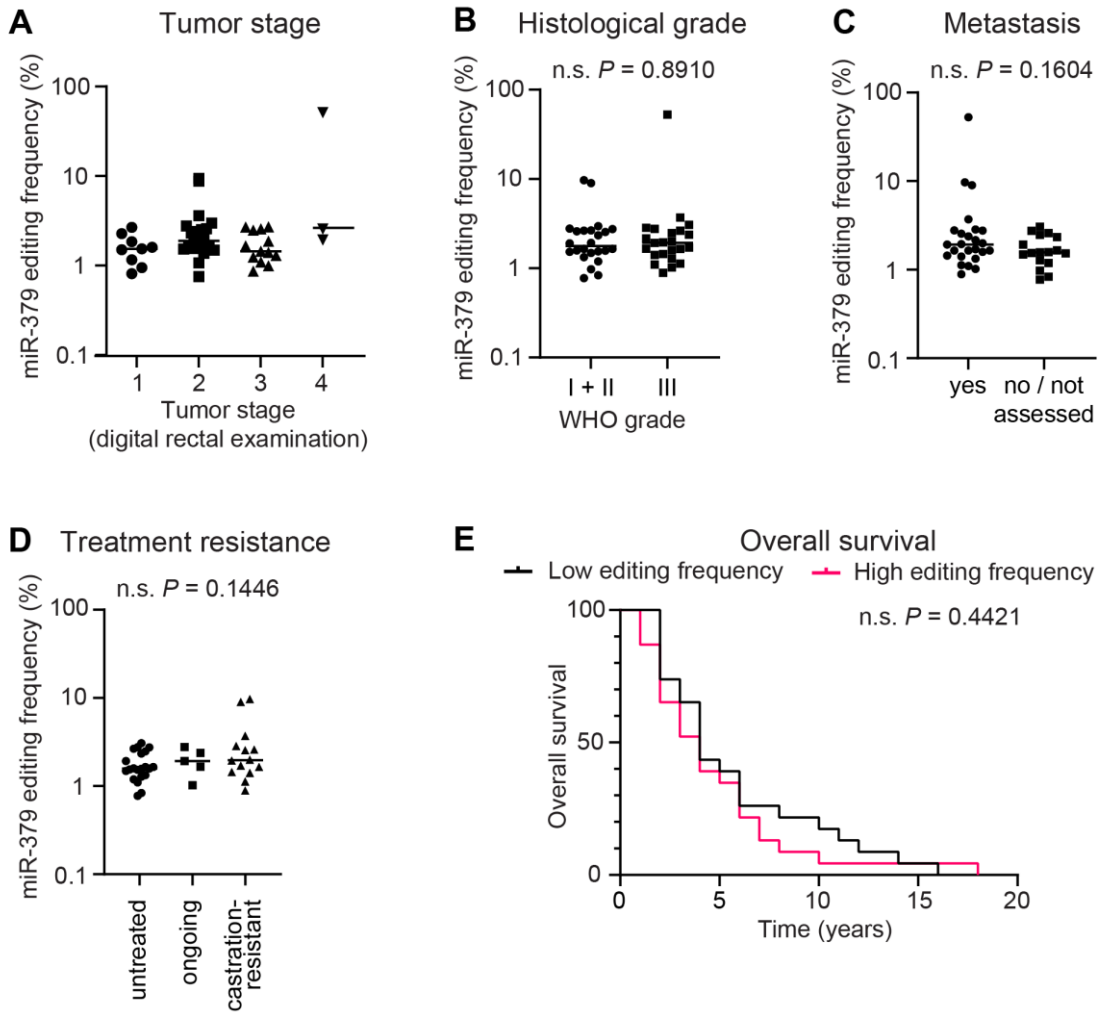

Supplemental Figure 10. Analyses of miR-379 editing frequency by (**A**) tumor stage (n = 9 for T1, n = 21 for T2, n = 13 for T3, n = 3 for T4), (**B**) histological grade (n = 4 for Grade I, n = 20 for Grade II, n = 23 for Grade III), (**C**) metastasis (n = 25 with metastasis, n = 17 without metastasis or not assessed), (**D**) androgen deprivation therapy (n = 14 hormone-naïve, n = 5 with ongoing hormone deprivation therapy, n = 21 castration-resistant), and (**E**) overall survival (n = 23 in each group). Editing frequencies were calculated based on the absolute number of edited miR-379 molecules divided by the sum of unedited and edited miR-379 molecules. Absolute numbers were derived from standard curves of serially diluted RNA oligonucleotides. Individual values and the median are shown. Group comparisons were done by Mann-Whitney U tests. For survival analysis, patients were divided at the median by editing frequency, and curves were compared using log-rank test. n.s. = not significant.

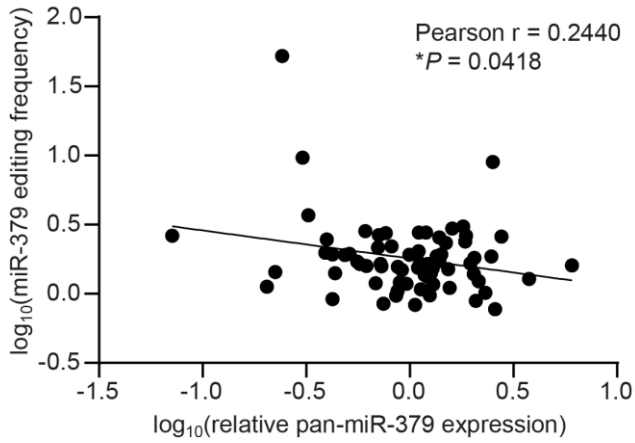

Supplemental Figure 11. Negative correlation between miR-379 editing frequency and relative pan-miR-379 expression in patient samples (n = 23). Both variables were log-transformed to enable meaningful linear regression and Pearson correlation.